

INFORMATION TO USERS

This material was produced from a microfilm copy of the original document. While the most advanced technological means to photograph and reproduce this document have been used, the quality is heavily dependent upon the quality of the original submitted.

The following explanation of techniques is provided to help you understand markings or patterns which may appear on this reproduction.

1. The sign or "target" for pages apparently lacking from the document photographed is "Missing Page(s)". If it was possible to obtain the missing page(s) or section, they are spliced into the film along with adjacent pages. This may have necessitated cutting thru an image and duplicating adjacent pages to insure you complete continuity.
2. When an image on the film is obliterated with a large round black mark, it is an indication that the photographer suspected that the copy may have moved during exposure and thus cause a blurred image. You will find a good image of the page in the adjacent frame.
3. When a map, drawing or chart, etc., was part of the material being photographed the photographer followed a definite method in "sectioning" the material. It is customary to begin photoing at the upper left hand corner of a large sheet and to continue photoing from left to right in equal sections with a small overlap. If necessary, sectioning is continued again — beginning below the first row and continuing on until complete.
4. The majority of users indicate that the textual content is of greatest value, however, a somewhat higher quality reproduction could be made from "photographs" if essential to the understanding of the dissertation. Silver prints of "photographs" may be ordered at additional charge by writing the Order Department, giving the catalog number, title, author and specific pages you wish reproduced.
5. PLEASE NOTE: Some pages may have indistinct print. Filmed as received.

Xerox University Microfilms

300 North Zeeb Road
Ann Arbor, Michigan 48106

73-25,218

DEMEL, John Tallev, 1942-
LOW TEMPERATURE HEAT CAPACITY OF YPb_3 , LaPb_3 ,
 La_5Pb_3 AND $\text{La}_5\text{Pb}_3\text{C}$.

Iowa State University, Ph.D. , 1973
Materials Science

University Microfilms, A XEROX Company , Ann Arbor, Michigan

Low temperature heat capacity of
 YPb_3 , LaPb_3 , La_5Pb_3 and $\text{La}_5\text{Pb}_3\text{C}$

by

John Talley Demel

A Dissertation Submitted to the
Graduate Faculty in Partial Fulfillment of
The Requirements for the Degree of
DOCTOR OF PHILOSOPHY

Major: Metallurgy

Approved:

Signature was redacted for privacy.

In Charge of Major Work

Signature was redacted for privacy.

For the Major Department

Signature was redacted for privacy.

For the Graduate College

Iowa State University
Ames, Iowa

1973

TABLE OF CONTENTS

	page
INTRODUCTION	1
SAMPLE PREPARATION	7
EQUIPMENT AND DATA ANALYSIS	21
RESULTS	24
YPb_3	24
LaPb_3	24
La_5Pb_3	28
$\text{La}_5\text{Pb}_3\text{C}$	30
Electrical Resistivities	30
DISCUSSION	34
Electronic Specific Heat Coefficients	34
Lattice Heat Capacity	36
CONCLUSIONS	48
BIBLIOGRAPHY	49
ACKNOWLEDGMENTS	52
APPENDIX	53

INTRODUCTION

In the last six years, eight of the seventeen rare earth-lead binary phase diagrams (1-9) have been investigated at the Ames Laboratory-USAEC, Iowa State University, Ames, Iowa. These investigations revealed a variety of intermetallic compounds in the different systems with the number and composition of the compounds varying from system to system. In addition several investigators (10-25) have determined the lattice parameters for many of the rare earth-lead compounds. This work has been summarized by Gschneidner and McMasters (26) who indicated trends in the data that point to occurrence or absence of certain compounds in the systems. Very little work has been done on these alloys other than the phase diagram determinations and crystal structure studies. The heat capacity measurements on the LaSn_3 and LaPb_3 compounds (AuCu_3 structure type) were performed by Bucher et al. (27) as part of an investigation of magnetic impurities in superconductors. Gambino et al. (17) determined the lattice parameters, superconducting transition temperatures and interatomic distances in the same compounds. The superconducting transition in YPb_3 was reported by Havinga (28) and Havinga et al. (29). In addition Havinga et al. (29) give values for the room temperature susceptibilities and thermoelectric power for YPb_3 and LaPb_3 .

The occurrence or nonoccurrence of some phases has been attributed to the influence of the 4f electrons in the lanthanide series (26). To support or refute this proposal such additional data are needed. In an effort to obtain some of these data heat capacity measurements were undertaken. Hopefully, this investigation is the first of a series of

studies which will provide a better understanding of these lanthanide compounds. The compounds chosen for this investigation were YPb_3 , LaPb_3 and La_5Pb_3 . After the heat capacities of these compounds had been measured the heat capacity of a fourth compound $\text{La}_5\text{Pb}_3\text{C}$ was measured to see if it would be helpful in understanding the La_5Pb_3 results.

Low temperature heat capacity measurements were chosen because they provide information about the vibrational and electronic behaviors of all materials and for some materials about their magnetic, crystal field and nuclear properties. At low temperatures (1-20°K) (30) the temperature dependence of the heat capacity of a normal, metallic material is as follows:

$$C_p = C_v = \gamma T + \beta T^3 = C_e + C_l. \quad (1)$$

C_e or γT is the electronic contribution and γ , the electronic specific heat constant, is proportional to the density of states at the Fermi energy $n(E_F)$. C_l or βT^3 is the lattice contribution and β is given by

$$\beta = \frac{12\pi^4 R}{5 \Theta_D^3} \quad (2)$$

if the heat capacity is given in units per g at. In Equation 2, R is the gas constant and Θ_D is the Debye characteristic temperature. The lattice term is the low temperature limit of the Debye model of a solid as an isotropic elastic continuum where the distribution of vibrational modes in the lattice is proportional to square of the frequency. Plotting data as C/T vs T^2 (i.e., dividing Equation 1 through by T) should yield a

straight line at low temperatures where the intercept is γ and the slope is β . Theoretically the Debye model should hold (i.e., Equation 1 is valid) up to temperatures of $\Theta_D^0/10$. But from the many heat capacity experiments that have been done it has been observed that the approximation is applicable in general only to temperatures up to 1/30th to 1/20th of the Debye temperature.

If an element or one of the elements in a compound has an unpaired inner electron, such as a 4f electron for the rare earth metals, and the material orders magnetically, then there is a magnetic contribution to the specific heat. This contribution according to simple spin wave theory has a $T^{3/2}$ temperature dependence for a ferromagnet or a T^3 dependence for an antiferromagnet. Furthermore, for compounds which contain a lanthanide element which has an unpaired 4f electron, additional contributions to the heat capacity may occur because of thermal excitation to higher electron (Schottky anomaly) or nuclear (nuclear hyperfine specific heat) energy levels.

At this initial stage of investigation the properties of rare earth-lead compounds, the electronic and vibrational characteristics, are of prime importance. Thus, because of the possibility of additional contributions to the heat capacity from compounds containing rare earths which have one or more unpaired 4f electrons, our study was limited to rare earth-lead compounds which contained scandium, yttrium, lanthanum or lutetium. The lanthanum compounds were selected because their lattice and electronic contributions to the heat capacities would be expected to be representative for the corresponding rare earth-lead compounds, and

later heat capacity investigations could deal with the magnetic contributions that arise with the filling of the 4f shell. Yttrium is similar to the heavy lanthanides in size but not in mass and this is important when considering the Debye temperature. It would have been better to have measured LuPb_3 as a typical representative of the heavy rare earth metals but unfortunately this compound does not exist. YPb_3 does, however, provide some interesting discussion when it is compared to LaPb_3 .

The 5:3 and 1:3 (rare earth to lead ratio) compounds were chosen because they represented the most frequently occurring compounds in the trivalent rare earth-lead systems, they were the compounds of lowest and highest lead composition and in most systems they were the compounds with the highest (5:3) and lowest (1:3) melting points.

The structure and lattice parameters for YPb_3 (22,25) and LaPb_3 (5,16,17) have been reported previously. These two compounds have the cubic AuCu_3 structure with the rare earth atoms located at the corners of the cube (0,0,0) and the lead atoms on the faces ($1/2,0,1/2$; $1/2,1/2,0$; $0,1/2,1/2$). Gschneidner and McMasters (26) reported lattice parameters for these compounds of $\underline{a}_0 = 4.818 \pm .005 \text{ \AA}$ and $\underline{a}_0 = 4.904 \pm .002 \text{ \AA}$ respectively.

La_5Pb_3 has the hexagonal $D8_8$ or Mn_5Si_3 type structure with $\underline{c}/\underline{a} < 1$ (5,10), and lattice parameters of $\underline{a}_0 = 9.526 \pm .002 \text{ \AA}$ and $\underline{c}_0 = 6.994 \pm .001 \text{ \AA}$ (26). The lanthanum and lead atoms are located in the following positions in the unit cell:

La(1): 4 d	$1/3, 2/3, 0; 2/3, 1/3, 0; 1/3, 2/3, 1/2; 2/3, 1/3, 1/2.$
La(2): 6 g	$x, 0, 1/4; 0, x, 1/4; \bar{x}, \bar{x}, 1/4; \bar{x}, 0, 3/4; 0, \bar{x}, 3/4$ $x, x, 3/4.$
Pb: 6 g	as above.

Hohnke and Parthé (31) in their paper on the $D8_8$ rare earth-bismuth-copper compounds pointed out that the lattice could be constructed of octahedra formed by surrounding each bismuth (lead) atom with six rare earth atoms and stacking these octahedra in the c direction. They also pointed out that the distances between the rare earth atoms in the $4d$ positions in the c direction were less than the metallic radii derived from the pure elements. They found that the rare earth and bismuth atoms occupied the positions noted above for the lanthanum and lead atoms respectively. When they added copper atoms to the structure these atoms went into the "holes" in the lattice at $0,0,0$ and $0,0,1/2$ or the $2b$ sites. The addition of the atoms caused the a lattice parameter to expand, but the c lattice parameter remained constant within a few thousandths of an angstrom. This particular structure was referred to as the "filled" $D8_8$ structure which had been reported earlier by Reiger et al. (32) for the Hf_5Sn_3Cu compound. Nowotny and Benesovsky (33) in a review article refer to this structure as being made up of octahedra of 6 atoms surrounding the atom in the $2b$ site.

It is proposed that the La_5Pb_3C compound has this "filled" $D8_8$ structure although it has not been reported in the literature. Extrapolated lattice parameters obtained from X-ray powder patterns show that the

carbon atoms do not distort the structure appreciably, but neutron diffraction data would be needed for absolute proof that the carbons are in the 2b positions.

SAMPLE PREPARATION

All samples used in this investigation were prepared by casting weighed amounts of the pure metals in tantalum crucibles. The rare earths were produced here at the Ames Laboratory by calcium reduction of the rare earth trifluorides. The lead used was purchased from Comnico Products, Co. The carbon used in preparing $\text{La}_5\text{Pb}_3\text{C}$ was spectroscopically pure carbon and its analysis is listed in Table 1 along with those of the rare earths and lead. The rare earths are listed by batch number and the impurities are listed in ppm atomic.

The congruently melting compounds, La_5Pb_3 and LaPb_3 , were heated inductively, inverted, heated again for at least three cycles and then heat treated below the lowest peritectic or eutectic horizontal adjacent to the compound in order to insure homogeneity. The photomicrographs, Figures 1, 2 and 3, show that the resultant alloys are essentially single phase compounds. YPb_3 presented more problems because it is a peritectically melting compound. The component metals were heated inductively to the liquid range, cooled and heated again. Each time the sample was held in the liquid range for about 30 min. This cycle was repeated three times and instead of slow cooling on the last cycle the sample was quenched by turning off the power to the induction coil and back filling the vacuum system with argon. After heat treating the sample for more than three weeks at 25°C below the melting point of 740°C , the peritectic structure disappeared leaving an essentially one phase alloy with only a small amount of second phase (see Figure 4).

Since preliminary measurements on La_5Pb_3 suggested that the Debye

Table 1. Chemical analysis of components (impurity levels are given in atomic ppm)

Impurity	Starting Materials						C	Pb
	La JC-1-112	JC-2-14	JC-4-79	LA-6471	Y JC-1-101	JC-3-4		
H	2	18	444	6	19	- ^a	-	-
Li	-	-	-	< .01	-	-	-	-
Be	0.4	≤ 0.2	0.1	≤ .05	-	< 1	-	-
B	0.3	≤ 0.1	-	0.3	-	0.5	-	-
C	625	486	90	254	650	ND	M ^b	-
N	8	193	77	41	18	50	-	-
O	40	219	682	203	1000	600	-	-
F	12	5	80	10	6	4	-	-
Na	2	10	40	-	2	10	-	-
Mg	2	5	0.3	≤ 0.1	20	4	0.6	0.1
Al	20	6	6	2	50	30	0.4	ND
Si	70	10	17	1	-	20	0.4	0.1
P	1	< .1	0.03	< 0.1	-	0.2	-	-
S	≤ 10	< 4	-	0.6	-	0.5	-	-

^a - not analyzed for.

^b M major component.

∞

Table 1. (Continued)

Impurity	Starting Materials						C	Pb
	La					Y		
	JC-1-112	JC-2-14	JC-4-79	LA-6471	JC-1-101	JC-3-4		
Cl	30	4	60	4	20	10	-	-
K	10	10	1	0.2	3	3	-	-
Ca	4	4	3	0.2	4	2	-	-
Sc	0.5	< 2	0.3	<u>≤</u> 0.1	3	10	-	-
Ti	15	1	4.0	1.0	-	0.1	-	-
V	0.2	0.2	-	0.08	30	0.5	-	-
Cr	0.7	3	10	0.3	50	10	-	ND
Mn	0.2	2	0.2	0.03	2	0.1	-	ND
Fe	40	30	1.6	5	318	< 200	0.6	0.1
Co	0.4	0.1	0.5	< 0.08	80	0.2	-	-
Ni	30	3	2.0	0.9	80	20	-	ND
Cu	5	3	5	0.5	20	20	-	0.2
Zn	0.2	0.8	0.4	0.07	8	0.2	-	-
Ga	ND	< 1	-	-	-	<u>≤</u> 0.05	-	-
Ge	ND	< .1	-	< 0.2	-	<u>≤</u> 0.1	-	-
As	ND	< .1	-	< 0.04	-	<u>≤</u> 0.02	-	-
Se	ND	< 0.1	-	< 0.06	-	ND	-	-
Br	0.4	< 0.6	-	0.1	-	< 0.1	-	-

Table 1. (Continued)

Impurity	Starting Materials						C	Pb
	La JC-1-112	JC-2-14	JC-4-79	LA-6471	Y JC-1-101	JC-3-4		
Rb	ND	ND	-	< 0.04	-	ND	-	-
Sr	ND	ND	-	< 0.06	-	ND	-	-
Y	4	0.2	3	2.0	M	M	-	-
Zr	1	≤ 0.1	ND	< 0.4	-	ND	-	-
Nb	≤ 5	≤ 40	-	-	-	≤ 5	-	-
Mo	7	-	ND	< 2	-	ND	-	-
Tc	-	-	ND	-	-	ND	-	-
Ru	ND	-	ND	< 1	-	ND	-	-
Rh	ND	-	ND	< 0.2	-	2	-	-
Pd	ND	-	ND	< 0.4	-	ND	-	-
Ag	ND	8	ND	< 0.1	-	ND	-	0.1
Cd	ND	-	ND	< 0.1	-	ND	-	ND
In	ND	-	ND	< 0.08	4	ND	-	ND
Sn	0.3	-	ND	< 0.4	-	ND	-	ND
Sb	ND	-	ND	< 0.08	-	ND	-	ND
Te	ND	-	ND	< 0.1	-	ND	-	-
I	ND	0.06	ND	< 0.06	-	ND	-	-
Cs	ND	-	ND	< 0.04	-	ND	-	-
Ba	ND	-	ND	< 2	0.3	ND	-	-

Table 1. (Continued)

Impurity	Starting Materials						C	Pb
	La					Y		
	JC-1-112	JC-2-14	JC-4-79	LA-6471	JC-1-101	JC-3-4		
La	M	M	M	M	40	1	-	-
Ce	≤ 10	10	30	27	90	0.6	-	-
Pr	≤ 20	30	3	2.2	4	0.2	-	-
Nd	≤ 10	10	40	1	8	1	-	-
Sm	4	< 0.6	-	< 0.3	1	ND	-	-
Eu	2	≤ 2	0.8	≤ 0.2	0	ND	-	-
Gd	4	≤ 1	30	1.0	50	4	-	-
Tb	2	≤ 3	0.3	0.9	20	1	-	-
Dy	ND	7	4	< 3	2	0.8	-	-
Ho	1	2	1	≤ 0.3	3	2	-	-
Er	1	1	1	1	30	1	-	-
Tm	ND	3	-	0.1	1	ND	-	-
Yb	2	< 1	.1	0.1	2	ND	-	-
Lu	5	3	-	≤ 2	9	1	-	-
Hf	≤ 2	-	-	< 0.8	9	ND	-	-
Ta	≤ 70	15	10	9	100	3	-	-
W	20	-	-	≤ 40	-	10	-	-
Re	ND	-	-	< 1	-	ND	-	-

Table 1. (Continued)

Impurity	Starting Materials						C	Pb
	La JC-1-112	JC-2-14	JC-4-79	LA-6471	Y JC-1-101	JC-3-4		
Os	ND	-	-	< 1	-	ND	-	-
Ir	ND	-	-	< 0.6	1	ND	-	-
Pt	ND	-	-	0.3	20	ND	-	-
Au	ND	-	-	0.1	3	ND	-	-
Hg	ND	-	-	0.2	3	ND	-	-
Tl	ND	-	-	< 0.1	-	ND	-	0.2
Pb	2	-	-	0.1	5	0.2	-	-
Bi	ND	-	-	< 0.08	1	ND	-	0.1
Po	-	-	-	< 0.2	-	ND	-	-
At	-	-	-	< 0.2	-	ND	-	-
Fr	-	-	-	-	-	ND	-	-
Ra	-	-	-	-	-	ND	-	-
Ac	-	-	-	-	-	ND	-	-
Th	3	-	-	-	-	ND	-	-
Pa	-	-	-	-	-	ND	-	-
U	ND	-	-	-	-	ND	-	-

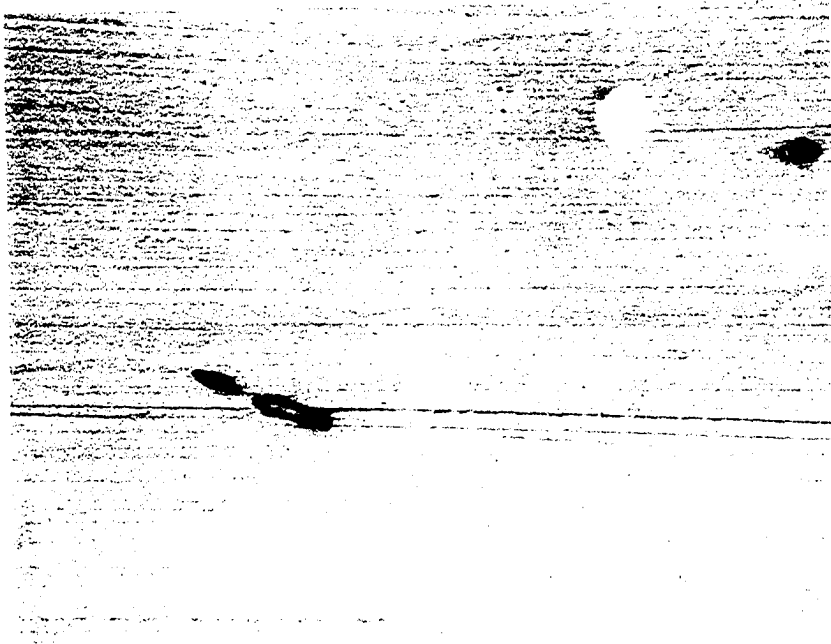


Figure 1. La₅Pb₃ I, mechanical polish, air etch.
Dark spots--voids, light spots--
probably La-La₅Pb₃ eutectic. X 250

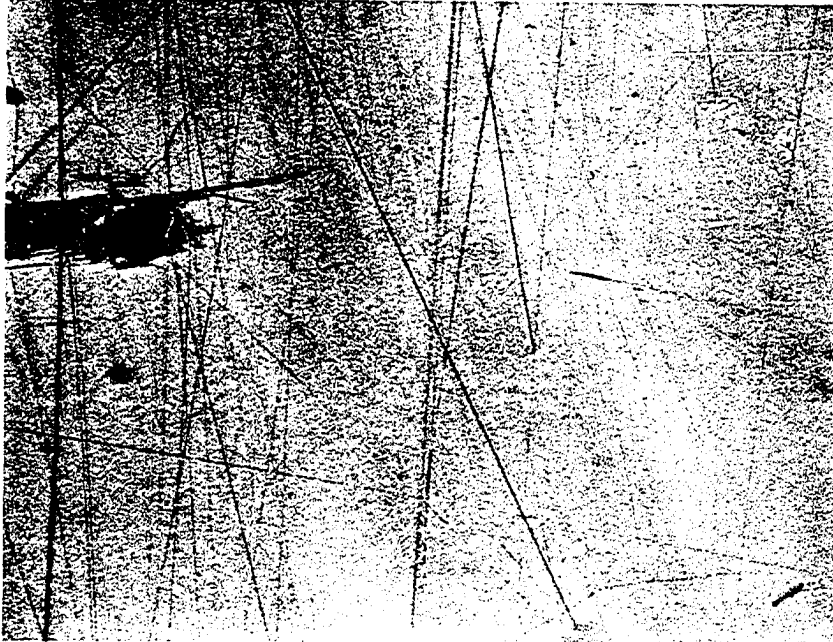


Figure 2. La_5Pb_3 II, mechanical polish, air etch.
Dark spots--voids, light spots--
probably La- La_5Pb_3 eutectic. X250

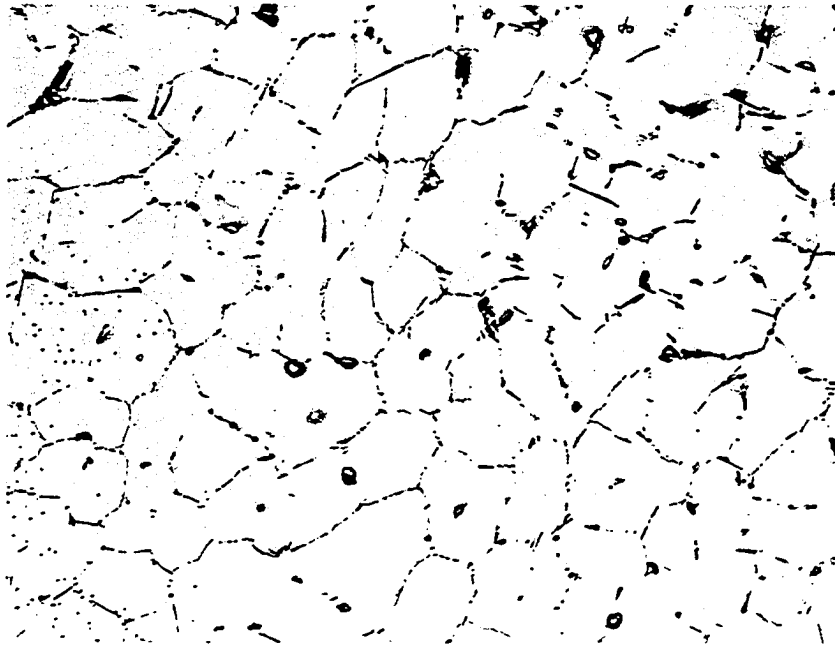


Figure 3. LaPb_3 , electropolished. Small spots--
probably Pb. X250



Figure 4. YPb₃, mechanical polish, air etch.
Small dark grey spots--probably YPb₂,
large black spots--voids. X250

temperature and its temperature dependence might be unusual, it was thought this might be associated with the vacancy in the 2b positions. Initial attempts were made to add sufficient copper to fill these two sites because Hohnke and Parthé (31) had reported rare earth-bismuth-copper compounds. Metallographic data indicated that only 60% of the copper was taken up by the La_5Pb_3 compound (i.e., $\text{La}_5\text{Pb}_3\text{Cu}_{0.6}$) and the excess copper formed a second phase. The lattice parameters reported for the rare earth-bismuth compounds are smaller than the lattice parameters for the rare earth-lead compounds and thus it seems likely that Hohnke and Parthé (31) actually prepared the 5:3:X(X<1) rare earth-bismuth-copper compounds. The addition of carbon was tried next and metallographic data indicated that all the carbon to make $\text{La}_5\text{Pb}_3\text{C}$ is taken up by La_5Pb_3 and no second phase material was present in the sample. The $\text{La}_5\text{Pb}_3\text{C}$ compound was prepared in much the same manner as La_5Pb_3 . The difference was that during the last cooling process the temperature was lowered in 20 C increments from 1510 C, the melting point, to approximately 1200 C. This procedure was followed because the differential thermal analysis used to determine the melting point suggested one or two transitions between 1500 C and 1200 C before the sample was homogenized. The microstructure is shown in Figure 5.

All the samples reacted rapidly with the atmosphere although the samples with the 1:3 structure reacted less rapidly than the samples with the 5:3 structure. Hohnke and Parthé noted that the bismuthides with copper in the 2b holes were more stable than those without the copper. In fact the addition of copper stabilized some lattices that would not form



Figure 5. $\text{La}_5\text{Pb}_3\text{C}$, mechanical polish, air etch. Photomicrograph taken through glass and methyl alcohol. The surface texture is the reaction of the sample with the alcohol. Large dark spots are pits in the surface. X250

unless copper was present. Here, the increase in the melting point for the 5:3:1 compound (1510 C) over the 5:3 compound (1450 C) shows that carbon also stabilizes the structure. However, it does not appreciably reduce the rate at which the atmosphere attacks the samples. As with the bismuthides the addition of copper to the rare earth-lead compounds did reduce the rate of oxidation. The samples were brittle and to get them out of their crucibles both ends of the crucible were cut off and then the tantalum was cut with a jeweler's saw along the entire length of the crucible. The remaining tantalum was peeled away from the sample. The processes of getting the sample out of the crucible, weighing the sample, and mounting the sample in the calorimeter addenda were performed in a helium filled drybox. The sample and addenda were then carried to the calorimeter in a helium filled, sealed jar. Mounting the sample and addenda in the calorimeter had to be done in the room atmosphere, but this took only five minutes or less and the reaction of the samples with the atmosphere was kept to a minimum.

The lattice parameters for the compounds prepared in this investigation are listed in Table 2 along with a summary of data from this and previous investigations. It is interesting to note that the addition of carbon to the lattice causes the c parameter to increase slightly (.023 Å) whereas the work on the bismuthides quoted above showed that copper caused the a parameter to increase (.083 Å).

Table 2. Data available for YPb_3 , LaPb_3 , La_5Pb_3 and $\text{La}_5\text{Pb}_3\text{C}$

Compound	YPb_3	LaPb_3	La_5Pb_3	$\text{La}_5\text{Pb}_3\text{C}$
Melting point ($^\circ\text{C}$)	740 ²	1160 ⁵	1450 ⁵	1510
Crystal structure	Cubic Cu_3Au L1_2	Cubic Cu_3Au L1_2	Hex. Mn_5Si_3 D8_8	Hex. $\text{Hf}_5\text{Sn}_3\text{Cu}$ Filled D8_8
Lattice parameters (\AA)	$a_0 = 4.8204 \pm 0.0002 \text{ \AA}$	$a_0 = 4.9028 \pm 0.0002 \text{ \AA}$	$a_0 = 9.532 \pm .002$ $c_0 = 6.974 \pm .003$	$a_0 = 9.531 \pm .003$ $c_0 = 6.997 \pm .002$
γ (mJ/g at. $^{-\circ}\text{K}^2$)	$2.32 \pm .77$	3.25^{27}	$0.81 \pm .55$	$1.53 \pm .31$
Θ_D° (K)	121	147^{27}	150	181
T_s (K)	$4.6(4.7 \pm .09^{29})$	4.1	--	--
Magnetic susceptibility χ (cm^3/g)	$0.11 \times 10^{-6}^{29}$	$0.165 \times 10^{-6}^{29}$	--	--
Thermoelectric power, S ($\mu\text{V}/^\circ\text{C}$)	4.2^{29}	1.4^{29}	--	--
Resistivity at R.T. ($\mu\Omega\text{-cm}$)	45	49	300	270

EQUIPMENT AND DATA ANALYSIS

The calorimeter used in this investigation is an adiabatic, pulse type and is described in detail elsewhere (34,35). The sample holder consists of two gold-plated copper plates held together by three gold-plated copper bolts. The samples were smeared with a low vapor pressure grease and mounted between the plates. Temperatures were measured using a Solition germanium resistance thermometer which was calibrated against another germanium resistance thermometer, GR618. GR618 was calibrated against a constant volume gas thermometer (36) and then was used to calibrate other germanium resistance thermometers at Iowa State University. A 1965 Calorimetry Conference Copper Standard (37) was used to check the accuracy of the calorimeter and it was found to be within one percent of the literature values for this standard. The precision of the copper standard was within approximately one percent, but precision of the data taken on the rare earth-lead samples studied in this investigation was not that good. Part of the problem was due to the difference in size of the standard and the samples. The copper standard weighed approximately 66 g while the samples varied in mass from about 10 to 30 g. This means that any uncertainty in the heat capacity of the addenda was increased and contributed to the problem described in the next paragraph.

The data was originally analyzed by the extrapolation of the temperature vs time curves before and after each heat pulse as described by Joseph (35) with the additional specification that a period of approximately four minutes is allowed to lapse after the heat pulse to start the

extrapolation (38) to determine the mid-point temperature of the heat pulse. The waiting period was to allow the sample and addenda to come to equilibrium. It turned out, however, that this waiting period produced extrapolated temperatures that were lower than they were if the extrapolation procedures were begun right after the heat pulse. This problem was magnified because the resistance of the thermometer changes exponentially with temperature but the extrapolation procedure assumes it to be essentially linear. The solution was to start the extrapolation immediately after the heat pulse to find the mid-point temperature for the data points below about 5-7 K (depending on the size of the sample), and to use smaller heat pulses so that the time for the sample to come to equilibrium would be kept to a minimum. This revised procedure was checked by running pulses of different sizes. The size of the pulse did not make any difference in the results as long as it was kept to a minute or less. Furthermore, the data obtained by the old method of determining the mid-point temperatures resulted in considerable scatter of the data points in the C/T vs T^2 plot. The revised method yielded C/T vs T^2 plots with considerably less scatter. This solution did not provide the most desirable precision but did allow for the data to be analyzed successfully. The points above the 5-7 K range were found to require the usual equilibration time and were handled in the manner described first above.

The $\text{La}_5\text{Pb}_3\text{C}$ sample was the last sample investigated and it was mounted in the addenda two different ways to see if the precision and accuracy of the data could be improved. The first way was as described above and the second way was to wrap the sample in copper foil and grease

to speed up temperature equilibration in the sample. The scatter in the data was less when wrapped with foil and these are the data reported in the results section.

After the heat capacities had been measured portions of the heat capacity samples were used in resistivity measurements. To do this a special holder was constructed to be used with existing resistivity equipment. It was built so that small pieces of the brittle samples could be measured without extensive sawing, cutting or filing which cause the samples to break in small pieces. Spark cutting, normally used for cutting brittle samples to desired shapes, is done in an oil that reacts rapidly with all the lanthanide-lead alloys.

The holder designed was of the four probe type with space to accommodate samples with maximum dimensions of 1.26 cm long, 0.32 cm high and 0.64 cm wide. The samples measured had dimensions that varied from 0.32 cm to 0.64 cm in width and 0.16 to 0.32 cm in height. The distance between voltage probes was 0.32 cm and the distance between current probes was 0.64 cm. Resistances were measured at 4.2 K, 78 K, and room temperature (~ 295 K). The accuracy of the measurements is limited by the lack of uniformity in the dimensions of the samples and the results could be expected to be only within 10 or 20 percent of the true value.

RESULTS



The heat capacity data from 2.7 to 19.3 K in the form C/T vs T^2 are plotted in Figure 6. A least squares fit of the data between 4.7 and 5.9 K gave values of $2.32 \pm .77$ mJ/g at. K^2 for γ and $1.09 \pm .03$ mJ/g at. K^4 for β which gives 121 ± 1 K for Θ_D . The narrow range for the fit is caused by a small change in slope at about 6 K. Fitting data above this range produced γ 's that decreased and became negative as more points were included in the fit. The superconducting transition temperature found here was between 4.55 and 4.7 K while Havinga et al. (29) quoted $4.72 \pm .09$ K. The variation of the Debye temperature as a function temperature was determined by assuming $C_1 = C - \gamma T$, and determining Θ_D from tables (30) of Θ_D/T vs $C/3R$. The effective Debye characteristic temperature, Θ_D^{eff} , decreased from 121 K at 5 K to 119 K at 9 K and then rose to 123 K at 19 K (Figure 7). This general shape is the same as those found for the other compounds studied in this investigation but the magnitude between the minimum and maximum points in the curve is quite different (see Figure 7). The heat capacity versus temperature data are tabulated in the Appendix in Table A(1).



The heat capacity of LaPb_3 was measured from 2.5 K to 20 K. The results are plotted in Figure 8 as C/T vs T^2 , and are listed in Table A(2) in the Appendix. The superconducting transition temperature, T_S , was found to be between 4.12 and 4.18 K in good agreement with previous work

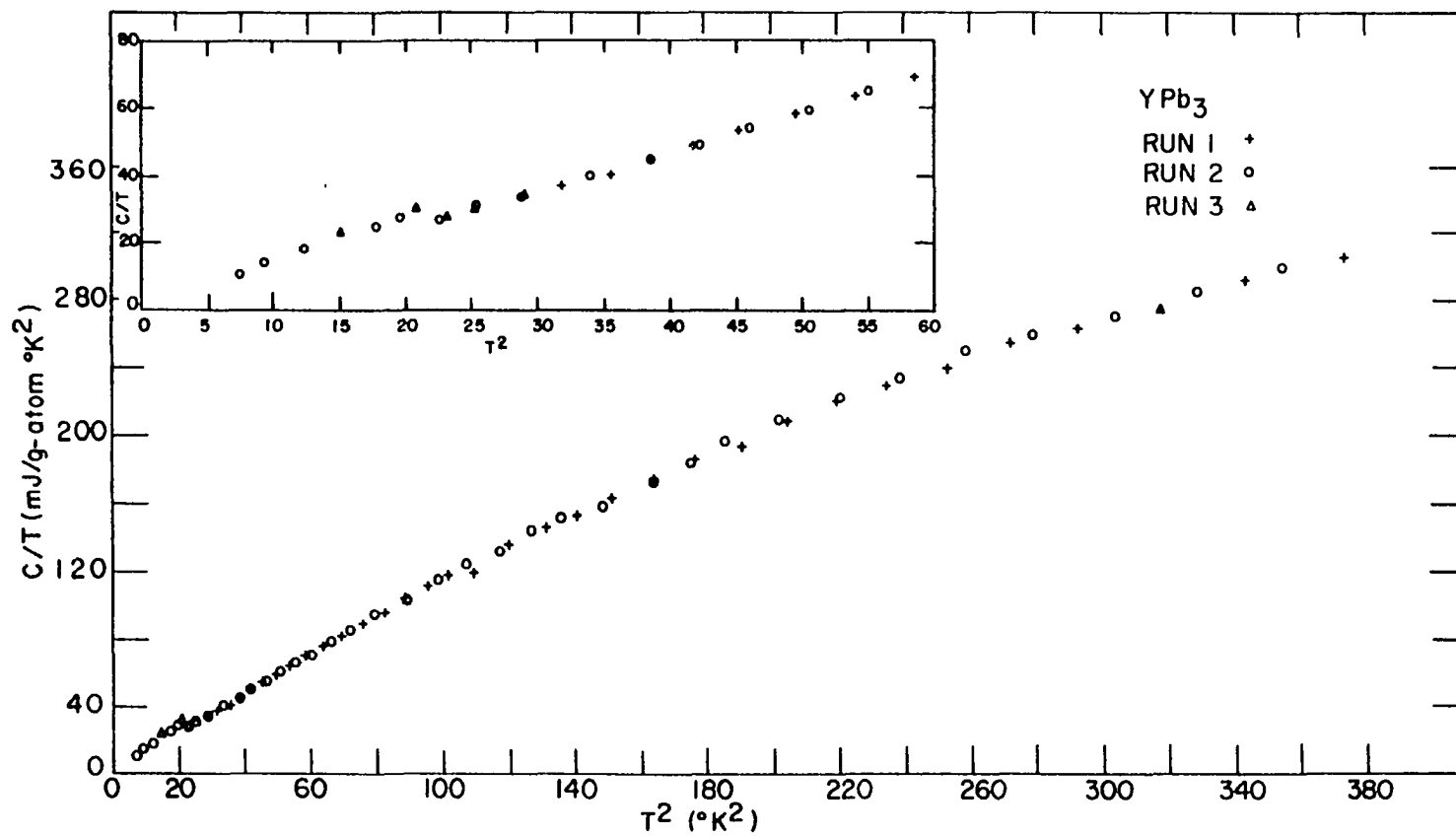


Figure 6. Heat capacity of YPb₃ from 2.7 to 19.3 K

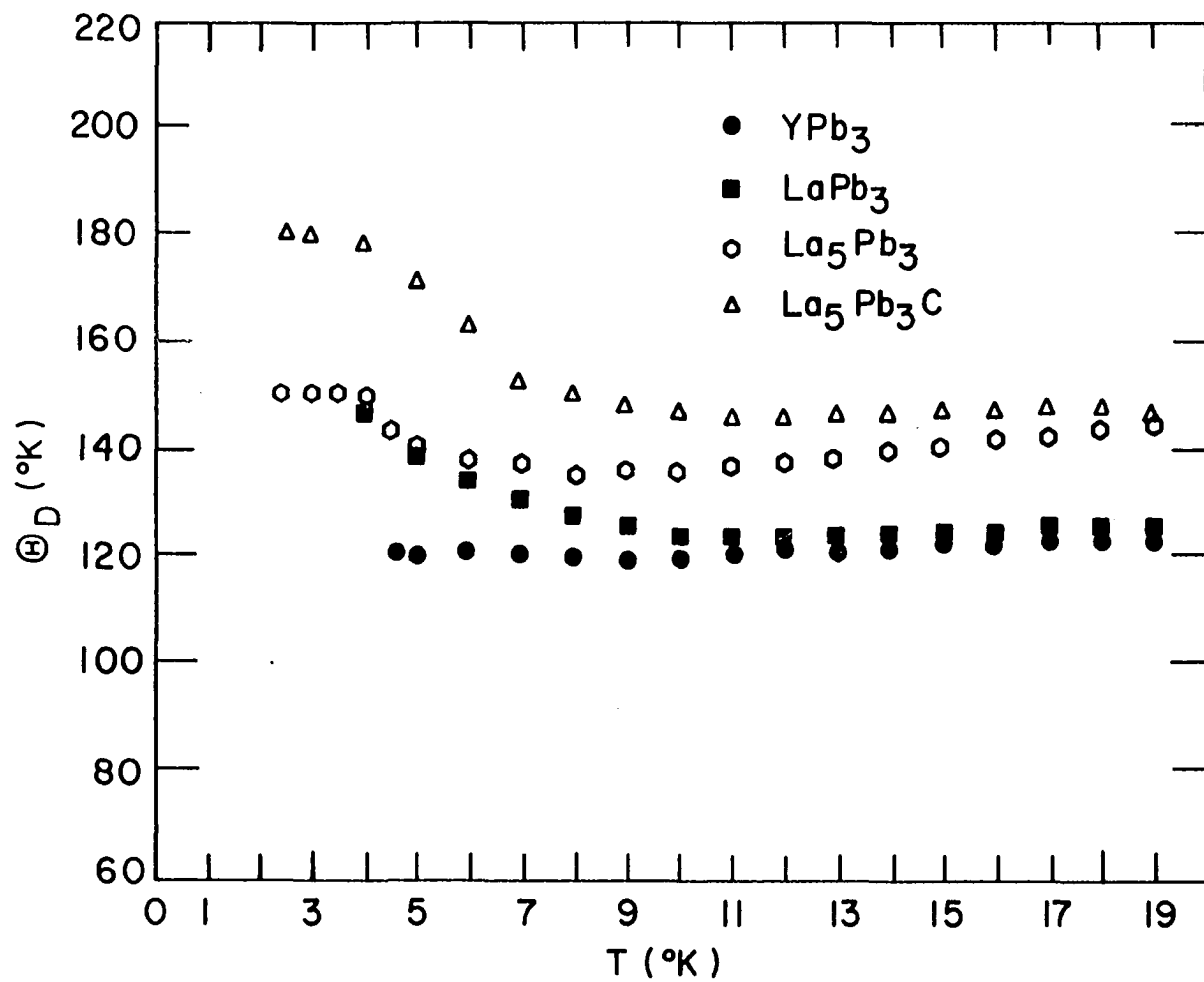


Figure 7. Effective Debye temperature from 2.5 to 20 K for YPb_3 , LaPb_3 , La_5Pb_3 and $\text{La}_5\text{Pb}_3\text{C}$

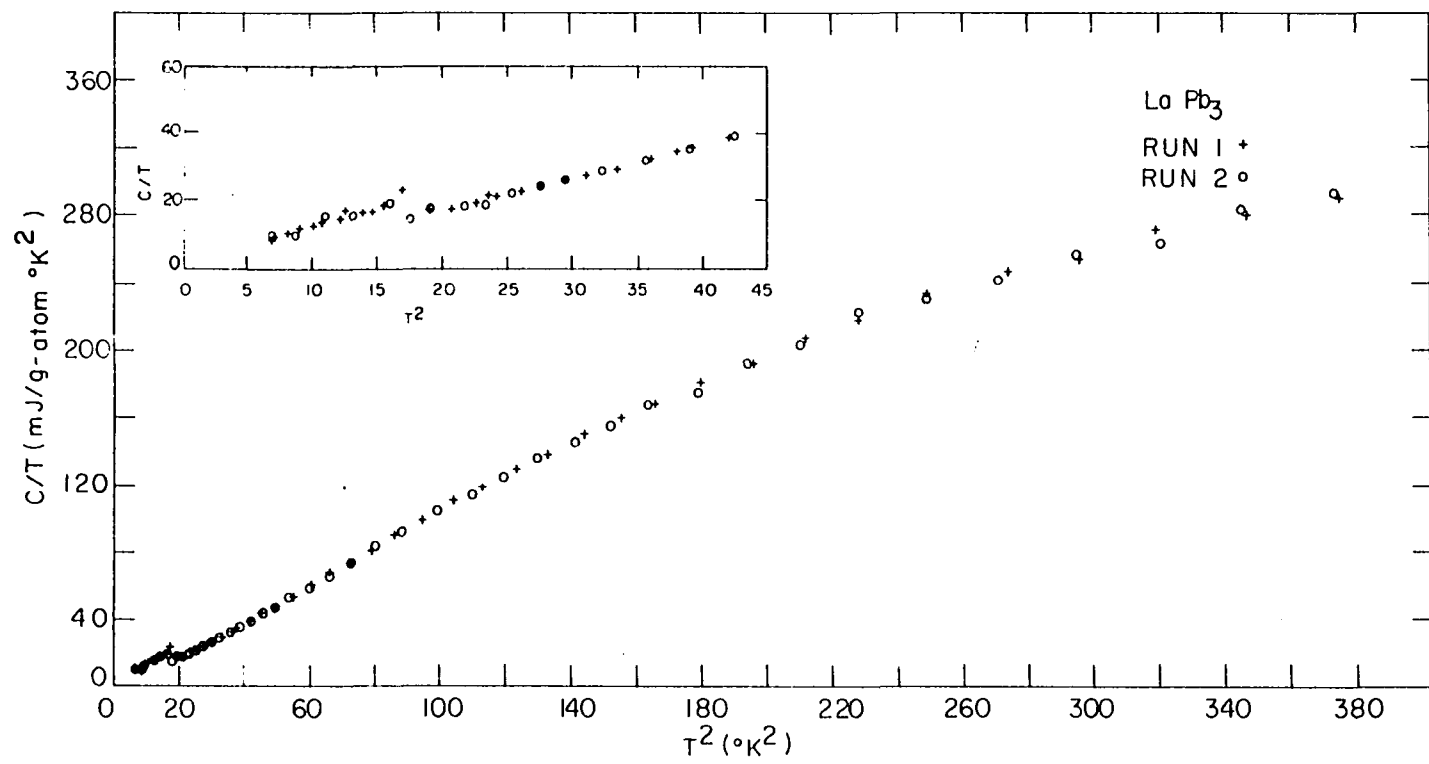
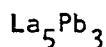


Figure 8. Heat capacity of LaPb₃ from 2.6 to 19.4 K

(27-29). Bucher et al. (27) measured the heat capacity at low temperatures in a magnetic field that was sufficient to suppress the superconducting transition temperature. Their results for γ and Θ_D were 3.25 mJ/g at. K² and 147 K, respectively. If the data (either ours or theirs) above T_s had been used to find γ and Θ it would have yielded values of $\gamma = \sim -0.6$ mJ/g at. K² and $\Theta_D \cong 122$ K. Θ_D^{eff} was found in the same manner as described for YPb₃ and the values are plotted against T in Figure 7. The Θ_D^{eff} varies from a value of 147 K at 4 K to a minimum of 124 K at about 12 K.



The C/T vs T² data for two La₅Pb₃ samples are shown in Figure 9 and the C vs T data are listed in the Appendix in Tables A(3) and A(4). Two samples were prepared because the data for the first one, La₅Pb₃ I, showed a considerable amount of scatter below 4 K and it was hoped that the data from the second sample, La₅Pb₃ II, might clarify the situation. Elimination of the scatter was quite important because the extrapolation of data above 4 K gives a negative γ . Once the scatter problem had been solved as described above data from both samples coincided. After the data was re-analyzed a least squares fit (from 2.5 to 3.9 K) gives $\gamma = 0.81 \pm .55$ mJ/g at. K², $\beta = 0.574 \pm .049$ mJ/g at. K⁴ and $\Theta_D = 150 \pm 5$ K. The Θ_D^{eff} vs γ plot shows that Θ_D^{eff} decreases from 150 K to a minimum of 136 K at 8 K and then rises to 145 K at 19 K.

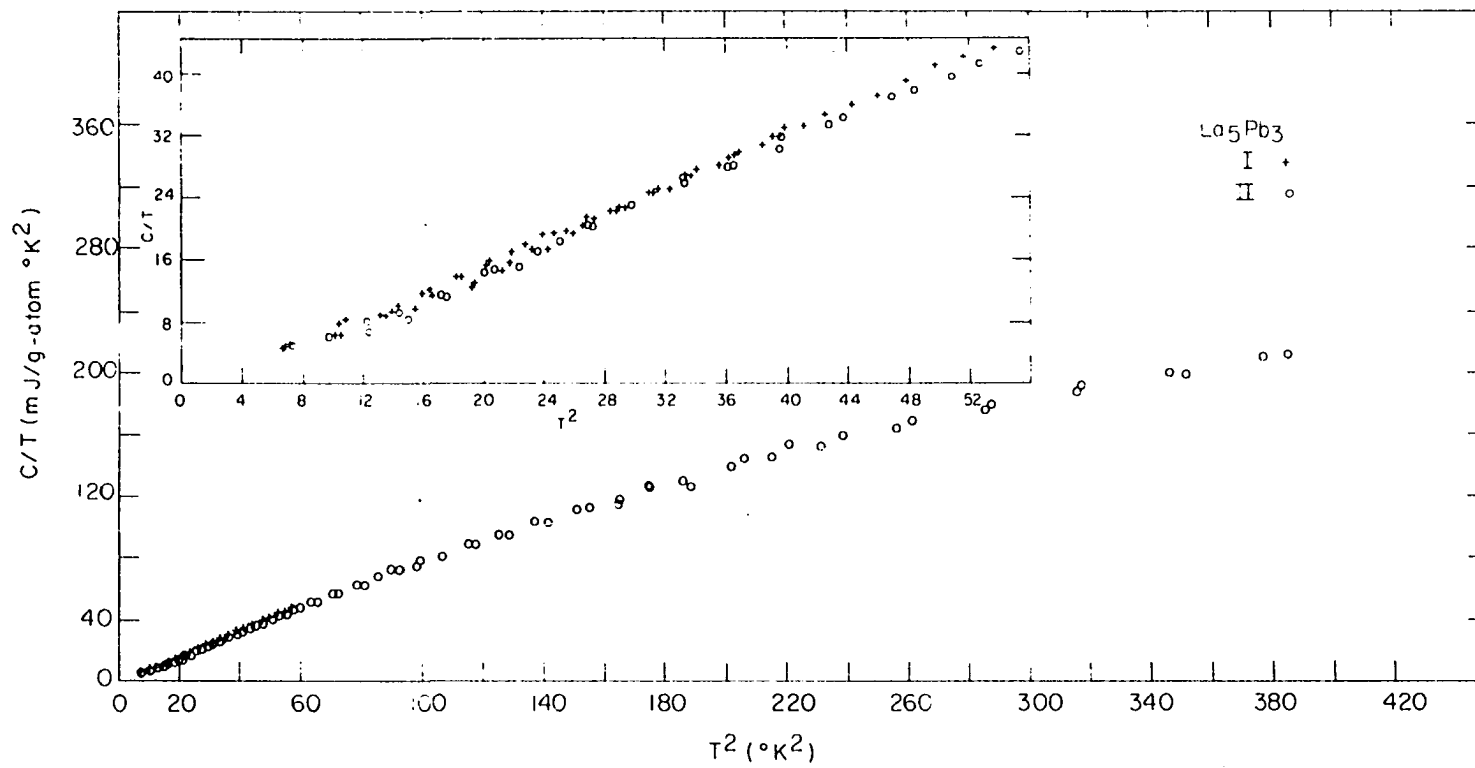
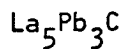


Figure 9. Heat capacity of La_5Pb_3 from 2.5 to 19.6 K



As noted in the section on Equipment and Data Analysis, this sample was measured twice. The second run, which resulted in data with significantly less scatter than the first run, was made with the sample wrapped in copper foil. This is consistent with the resistivity results, which show that the resistivity is higher for this compound than it is for the other compounds at 4.2 K (see the next section). Normally in metals the thermal conductivity is proportional to the electrical conductivity and if that is the case here it would explain the improved results with the sample wrapped in copper.

The heat capacity data are presented in Figure 10 (and in Table A(5) in the Appendix) in the form C/T vs T^2 . The break in slope for $\text{La}_5\text{Pb}_3\text{C}$ occurs at a higher value of T^2 than it does for La_5Pb_3 . The results from the least squares fit of the data between 2.5 and 4.3 K are $\gamma = 1.53 \pm .31$ mJ/g at. K² and $\beta = 0.328 \pm .024$ mJ/g at. K⁴ which gives $\Theta_D^0 = 181 \pm 4$ K. The data are also presented as Θ_D^{eff} vs T in Figure 7.

Electrical Resistivities

The room temperature resistivities measured for the compounds were 45, 49, 300 and 270 $\mu\Omega\text{-cm}$ for YPb_3 , LaPb_3 , La_5Pb_3 , and $\text{La}_5\text{Pb}_3\text{C}$, respectively. With the error in measurements being at least 10% the resistivity values for the LaPb_3 and YPb_3 compounds can be considered to be about the same. The same can be said for the 5:3 and 5:3:1 compounds. It is reasonable to say that the resistivity for the 1:3 compounds is about 1/6 of the resistivity for the 5:3 and 5:3:1 compounds. The temperature dependence of the electrical resistivity is best illustrated by a plot of

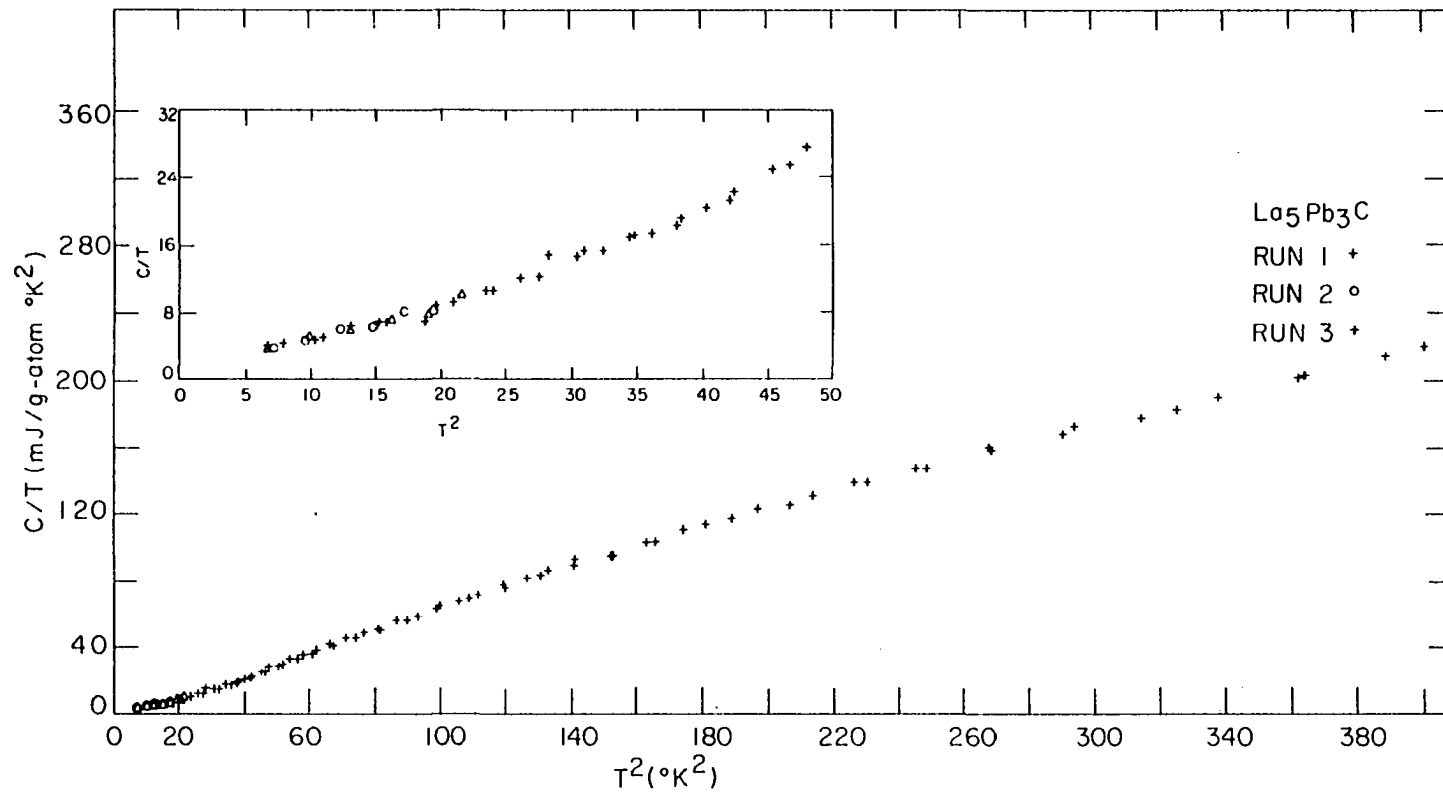


Figure 10. Heat capacity of La_5Pb_3C from 2.5 to 20 K

the reduced resistivity or ρ_T/ρ_{295} against the temperature, Figure 11.

It is noted that the values for YPb_3 , LaPb_3 , and La_5Pb_3 decrease rapidly with temperature in a manner expected for normal metallic conductors, while the values for $\text{La}_5\text{Pb}_3\text{C}$ decrease quite slowly. This will be discussed later.

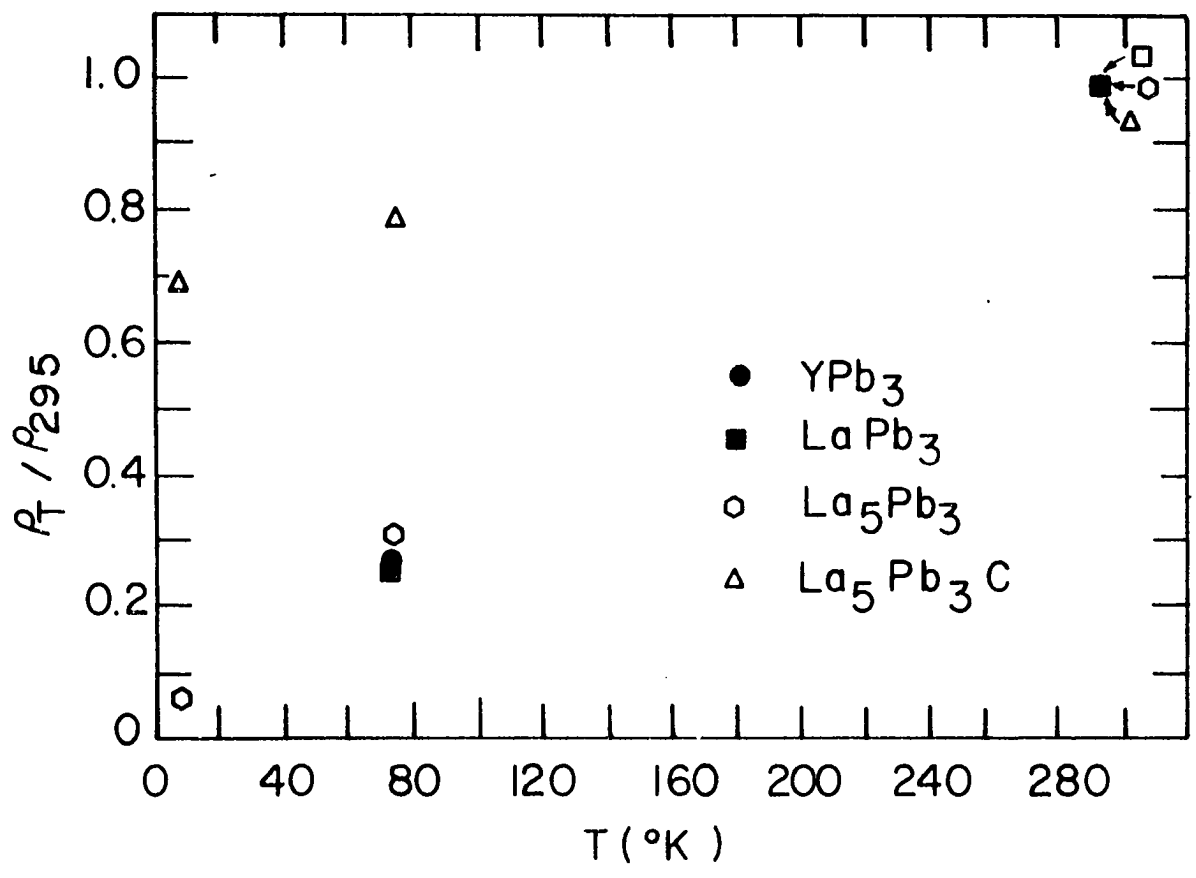


Figure 11. Reduced resistivities for YPb_3 , $LaPb_3$, La_5Pb_3 and La_5Pb_3C at 4.2, 78 and ~ 295 K

DISCUSSION

The lanthanum compounds studied in this investigation all deviate from Debye behavior at low temperatures as shown by the C/T vs T^2 curves. This presents problems both for the fitting of the curves and for using this data to predict how the rest of the rare earth-lead compounds will behave. In the following paragraphs the numbers obtained here will be compared with each other and with other data to see if they are consistent. Different models and methods of fitting the data will be used to achieve this end and also to see if the data obtained here will allow predictions about the magnitude of the properties of the other lanthanide-lead compounds.

Electronic Specific Heat Coefficients

There has been no heat capacity work for the 5:3 and 5:3:1 compounds in the lanthanide-lead systems and very little on the 1:3 compounds. Thus there is only a limited amount of information that can be used to cross check the results of this investigation.

Bucher et al. (27) measured the heat capacity for LaPb_3 both in the normal state and the superconducting state and showed that there was a change in the slope of the C/T vs T^2 curve at the superconducting transition temperature. Normally the slope of the curve stays constant above and below T_S when the heat capacity is measured in the normal state (30,35). The normal state data below T_S for LaPb_3 give a positive γ but that above T_S give a negative γ value, which is a physical impossibility. The data between the transition temperature and the first change in slope for

YPb₃ produce a positive γ . If the data above that first change in slope are used then the extrapolation to 0°K produces a negative γ as in the LaPb₃ compound. If data were taken for YPb₃ in the normal state below T_S then it is possible that there is another change in slope that occurs which would give both a different γ and a different θ_D .

To see if the γ values for these two compounds, YPb₃ and LaPb₃, are reasonable it is possible to use some of the data that Havinga et al. (29) have published. They measured the superconducting transition temperatures, the thermoelectric power and the susceptibilities of these two compounds. Both of the compounds are weak paramagnets and since the magnetic susceptibility for these kind of materials is proportional to the density of states at the Fermi energy as is the electronic specific heat constant one can check to see if the data are consistent with one another. The ratio of the susceptibilities (see Table 2) is 1:5 which compares very favorably to the ratio of the γ values (1.4). Thus these ratios lend credibility to the γ value found in this investigation for YPb₃.

Another parameter which also supports the γ value for YPb₃ is the ratio $\Delta C/\gamma T_S$ where ΔC is the change of heat capacity at T_S , and γ and T_S , are defined as above. According to BCS theory the above relation should be equal to 1.52. Experimentally it was found that $\Delta C/\gamma T_S$ equaled 2.16 and 1.97 for YPb₃ and LaPb₃ respectively. Again the closeness of these values indicates the γ value for YPb₃ is reasonable. These $\Delta C/\gamma T_S$ values are higher than values reported by Joseph et al. (39) and Hungsberg and Gschneidner (40) for other rare earth intermetallic compounds which had

values equal to or lower than the BCS theoretical value of 1.52. Assuming that the data obtained for YPb_3 are correct the γ values for the rest of the rare earth-lead 1:3 compounds should be expected to be less than or approximately equal to 3mJ/g at. K^2 .

The γ values for La_5Pb_3 and $\text{La}_5\text{Pb}_3\text{C}$ are both small, and within the experimental error limits they are the same. Although the effect of adding carbon to La_5Pb_3 appears to increase the density of states at the Fermi surface, the lack of precision prevents one from stating this conclusively. Before the problem with the data analysis was solved it appeared that these two compounds would have γ values ≈ 0 and thus might be semiconductors or semimetals. The resistivity measurements and also the γ values given herein, show that they are metallic materials with unfilled valence bands.

Lattice Heat Capacity

The Debye theory is based on the assumption that the vibrations of the lattice at low temperatures have a distribution, $g(\nu)$, which is proportional to the vibrational frequency squared, ν^2 . Unfortunately, as many heat capacity experiments have shown, this particular model fails because the distribution of vibrational modes $[g(\nu)]$ is not a smooth function of the frequency up to ν_{max} , but has some peaks and valleys. Normally, however, the model is found to hold in the low temperature range below $\Theta_D^0/30$.

For all four of the compounds investigated here a deviation from this model has been found, but fortunately there is a portion of the C/T vs T^2 plot which provides a straight line so that a least squares fit can be

made and a value for the limiting Debye characteristic temperature, Θ_D^0 , can be calculated.

Lindemann proposed a relation (41)

$$\left[\Theta_D^0 = k \left(\frac{T}{V^{2/3} M} \right)^{1/2} \right]$$

which takes into account the melting point of the compound or element, T , the mass per mole for elements or g at. for alloys, M , the volume per g at., V , and the Debye temperature, Θ_D^0 , and for compounds that are isostructural the constant of proportionality, k , should be the same. There is another relation which can be used to compare Θ_D^0 values but it does not take into account the melting point and molecular volume of the compound but does take into account the difference in mass between two compounds. This relation says that the product of Θ_D^0 and the square root of the mass should be constant for isostructural compounds. Table 3 lists the values for the proportionality constant for the Lindemann relation and the product $\Theta_D^0 \sqrt{M}$.

As can be seen from Table 3 the values of k for LaPb_3 and YPb_3 (165 and 154, respectively) differ as much as might be expected for these similar compounds. Perhaps the large difference in melting points (740 K- YPb_3 and 1160 K- LaPb_3) and the mode of melting (YPb_3 melts incongruently and LaPb_3 melts congruently) account for this 8% difference. Even though these relations show that there seems to be large differences between the product $\Theta_D^0 \sqrt{M}$ using the Debye temperature from the low temperature slope of the C/T vs T^2 plot, the Θ_D^{eff} vs T plot (Figure 7) shows that LaPb_3 and YPb_3 have almost the same Debye temperature at temperatures

Table 3. Comparison of the compounds using standard relations

Compound	Mass/Mole	Mass/g at.	\sqrt{M}	$\frac{e_D^0}{D}$	$\frac{e_D^0}{D}\sqrt{M}$	$k_{\text{Lindemann}}$
YPb_3	710	178	13.34	121	1609	154
LaPb_3	760	190	13.79	147	2027	165
La_5Pb_3	1316	164	12.82	151	1935	191
$\text{La}_5\text{Pb}_3\text{C}$	1328	148	12.14	180	2197	205

above 12K. Thus when the product of $\Theta_D^{\text{eff}}\sqrt{M}$ from the higher temperature region is used the values have a difference of only 9% whereas the low temperature values of $\Theta_D^0\sqrt{M}$ differ by about 25%. In the Lindemann relation the agreement is enough better that it indicates that the melting point of the compounds should not be overlooked when comparing Debye temperatures of closely related solids. Both of these relations give reasonable confirmation to the calculated Θ_D^0 for YPb_3 .

Using these two relations to compare the Debye temperatures for the 5:3 and 5:3:1 compounds probably is not good practice because there is a difference in the structures. In the 5:3:1 compound with the carbon in the "holes" the vibrational distribution would be expected to be different than that for the 5:3 compound and the Debye temperature would also be different. There is a difference in the Debye temperatures from the straight portion of the C/T vs T^2 curves, but the plot of effective Debye temperatures (Figure 7) shows that at 20 K the two lattices have the same Θ_D^{eff} . Also the general shape of the two curves is different. Where the La_5Pb_3 curve has a definite minimum and begins to increase again, the $\text{La}_5\text{Pb}_3\text{C}$ compound has a Θ_D^{eff} curve that drops from a high value at low temperatures to a lower value and then stays constant throughout the temperature range investigated. The Lindemann constants for the two compounds with the $D8_8$ structure do not agree and neither do the products of the Debye temperature times the square root of the mass. The differences are 7% and 12% respectively, which is less than the differences for the two AuCu_3 type structures. However, one might have expected the differences for the AuCu_3 structures to be less.

The deviations of the effective Debye temperatures from a horizontal line (Figure 7) indicate that the Debye approximation does not hold with the exception, perhaps, of the YPb_3 lattice. The fit for YPb_3 may deviate if the heat capacity measurements would be taken at temperatures lower and higher than measured here. Knowing that the Debye approximation does not work the logical approach was to see if there would be some model that would fit the temperature dependence of the specific heats for the La_5Pb_3 and $\text{La}_5\text{Pb}_3\text{C}$ compounds.

Because the lanthanum atoms in the 4d positions are closer together than their normal metallic state it was thought that a model originally proposed by Tarassov and successfully applied by deSorbo (42) to antimony, selenium and tellurium might fit the heat capacities for the 5:3 and 5:3:1 compounds. Basically Tarassov suggested that if layers of a structure were further apart than the atoms within a layer then the lattice contribution of the specific heat could be expressed as a sum of two terms. The first would be a two-dimensional Debye lattice for the vibrations within the layers or planes and the second would be a three dimensional Debye lattice for the interlayer vibrations. For a solid which contains a chain of atoms and where spacing between chains and spacing within chains varies, he suggested that the lattice contribution consisted of the sum of a one dimensional and a three dimensional Debye lattice. Thus for both kinds of solids two vibrational frequencies or effective characteristic temperatures were needed to explain the lattice heat capacities. Because there is the change in slope in the C/T vs T^2 plots for both D8_8 compounds it was felt that the low temperature data might represent one

vibrational frequency while the higher temperature data would represent the sum of the two frequencies.

In these cases both of Tarassov's models were tried. First the one with the one dimensional chains was tried because of the spacing between the atoms in the 4d sites, which form chains in the $D8_8$ compounds and then the model for the two dimensional layers was tried because the vibrations in the basal plane and the plane parallel to the basal plane at $Z = 1/2$ might be affected by the holes at the corners of the unit cells. Neither one worked. Any combination of the two vibrational frequencies that fit at low temperatures did very poorly at fitting the higher temperature data.

Further trials were carried out by using simple combinations of Einstein and Debye functions but these also failed. The same problem arose when fitting the heat capacity results by a power series equation, $C = AT + BT^2 + CT^3$. . . The higher temperature portion was fitted quite well but the errors for the points below the slope change (in the C/T vs T^2) plots were too large to be acceptable. For example the La_5Pb_3C data would fit within 2% for the temperatures above 5.5 K but the data below 5.5 K deviated from the fit by as much as 13%.

Because the various models did not work successfully and because the curves of Θ_D^{eff} vs T did not reveal more than the fact that the lanthanum-lead compounds did not follow the Debye approximation which the YPb_3 compound apparently came rather close to fitting, it was decided to try to treat the heat capacity data a different way.

Bijl (43) proposed another way of representing heat capacity data

because he felt that the effective Debye temperature plotted against T was not revealing much about the similarities and differences in different lattices. Most of his objections were for temperatures higher than the range covered here, but two of them were pertinent at all temperatures. The first is that presenting the data as a function of T rather than as a function of some reduced form of T , such as T/Θ_D^0 , does not allow compounds to be compared to each other. This objection can be dealt with easily by plotting Θ_D^{eff} as a function of T/Θ_D^0 . Some researchers do this but the standard form still seems to be Θ_D^{eff} vs T . He feels that his second objection is more important. Bijl found that fitting the data using the method described in the Results Section ($C - \gamma T = C_{\text{lattice}}$, then finding Θ_D^{eff} from the tables) produced curves of Θ_D^{eff} vs T in which Θ_D^{eff} is decreasing while the distribution function, $g(v)$, was actually found to be increasing faster than Debye's proposed $g(v) \equiv v^2$. What he wanted was a method of representing the specific heat data that would show the deviation of $g(v) \equiv v^2$ directly. Thus if the actual frequency distribution increased faster or slower than the Debye model the new representation should indicate that change directly.

He proposed calculating the Debye characteristic temperature from the low temperature slope of the C/T vs T^2 plot, Θ_D^0 , and then using this Debye temperature he found a theoretical value for the heat capacity of the lattice, C_{ℓ}^D , for every temperature from the tables of $C_{\text{lattice}}/3R$ vs Θ_D/T . This gives values of the expected Debye lattice heat capacity. The next step was to find the experimental value of the heat capacity of the lattice, C_{ℓ}^{exp} , for the corresponding temperature. The experimental value

of the lattice heat capacity is divided by the theoretical value and the resultant, C_{reduced} or C_r , value is plotted against T/θ_D^0 . In this way if the lattice was acting as a Debye lattice at all the temperatures investigated the value of C_r would equal 1.000 at all values of T/θ_D^0 . If the heat capacity of the lattice deviated from the Debye model, such that $g(\nu)$ increased faster or slower than the Debye model would have allowed, C_r would become greater than 1 or less than 1, respectively. The data for the four compounds investigated are shown in Figure 12. Bijl noted in his article that the peak in C_r for most elements was near $T/\theta_D^0 = 0.1$, but as the mass of the element or equivalently the mass per g at. in a compound or alloy become larger the peak in C_r shifted to a lower T/θ_D^0 value and became larger. The compounds studied here have peaks in C_r which occur at values of T/θ_D^0 ranging from 0.05 to 0.075.

At this point Bijl's observation about where the peak in C_r occurs seems to hold within the particular type of crystal structure, but does not appear to hold between structure types. For the compounds with a larger mass per g at. of the AuCu_3 structure type, i.e., LaPb_3 , a peak in C_r occurs at a lower T/θ_D^0 than the one for YPb_3 . The same is true for the La_5Pb_3 and $\text{La}_5\text{Pb}_3\text{C}$ compounds. Yet the peaks for both La_5Pb_3 and $\text{La}_5\text{Pb}_3\text{C}$, which have a smaller mass per g at., are at lower T/θ_D^0 than are the 1:3 compounds. His observation that the height of C_r increases as the mass increases holds only for the AuCu_3 structures but does not appear to hold for the D8_8 and filled D8_8 structures. Keep in mind that Bijl developed this representation for the elements and made his observations on the work that had been done up to the time that the paper was written and there

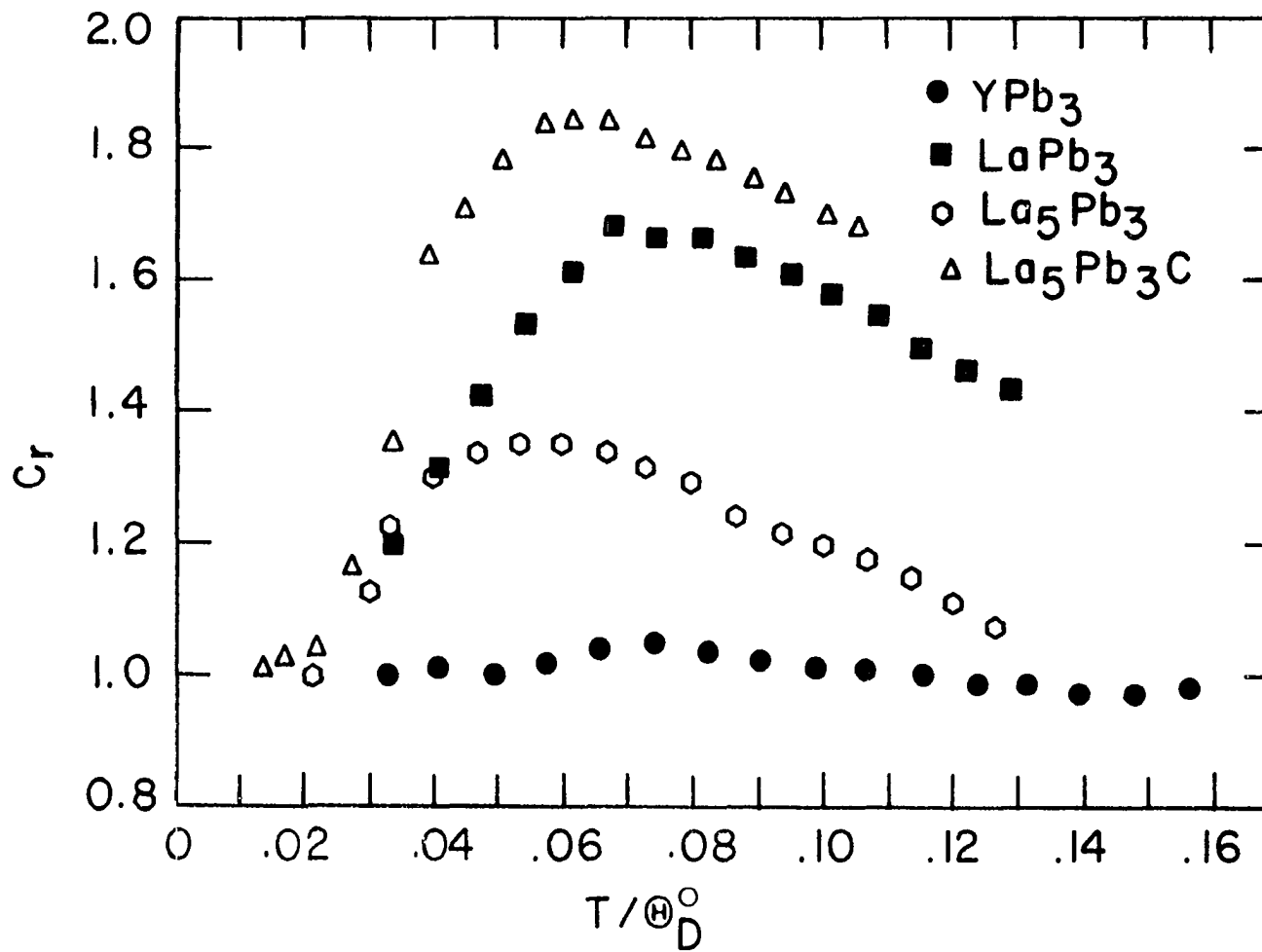


Figure 12. Reduced heat capacity for YPb_3 , $LaPb_3$, La_5Pb_3 and La_5Pb_3C plotted against T/Θ_D^0

were only a few metals investigated that had strongly anisotropic lattices.

Two of the elements that he observed that did have strongly anisotropic lattices were zinc and cadmium. Both of these elements had their peaks shifted to a value of $T/\Theta_D < 0.1$. This was felt to be due to the fact that the waves in the \underline{c} direction for these elements apparently are excited more easily than the lattice waves in the \underline{a} direction. Perhaps this is the key to the discrepancies noted above. The $D8_8$ lattice would be more likely to be anisotropic than would the $AuCu_3$ structure types for two reasons which were discussed in the Introduction: (1) the holes in the $D8_8$ structure which affect the vibrations of the atoms surrounding them, and (2) the atoms in the 4d positions which are closer to each other than in their pure metallic state and also closer together than the rest of the atoms in the structure. Therefore if the differences in anisotropy in the two types of lattices investigated here are considered, Bijl's representation and comments seem to be consistent with the exception of his explanations for peak height.

With this representation of the data as with previous calculations there seem to be discrepancies between the YPb_3 data and the $LaPb_3$ data. The YPb_3 data was almost a straight line while the $LaPb_3$ data had a definite peak. Bijl showed that elements with the same crystal structure and valence had reduced curves that were very similar. To see if this would be true for alloys three lanthanide-aluminum laves phase compounds, RAI_2 , were compared using this representation. Hungsberg's data for YAl_2 , $LaAl_2$ and $LuAl_2$ (44) were put in the reduced form and plotted. Although the

data was not sufficient to determine peak heights, the data for the three compounds fell almost on the same line. When the Lindemann constant for LaPb_3 was used to find a Θ_D^0 for YPb_3 and this Θ_D^0 was used in a reduced plot it provided a curve with the same shape as the LaPb_3 curve although the magnitudes were not as close as those of the RAl_2 compounds. The RAl_2 data implies that the same situation should hold for other series of compounds. Both LaPb_3 and YPb_3 are superconductors and the data from these two compounds is to be used to represent the lattice and electronic contributions to the heat capacity of normal trivalent RPb_3 alloys. The LaAl_2 compound is superconducting but the other two RAl_2 are not, yet their reduced curves are nearly the same. The only difference is that the LaAl_2 electronic specific heat constant is about twice those of YAl_2 and LuAl_2 . Knowing these facts it is reasonable to say that the lattice contribution from the LaPb_3 compound can be used to represent the other RPb_3 compounds but to use the LaPb_3 γ value for the other compounds would be questionable in view of the data for the RAl_2 compounds. It would be reasonable to use the La_5Pb_3 data to represent the lattice and electronic contributions to the heat capacity for the other trivalent R_5Pb_3 alloys.

The reduced form for one compound does appear to give the shape of the curve for the other isostructural compounds. Lindemann's equation based on one compound does give an approximate Θ_D^0 for the other isostructural compounds. Using the two together provides not only what the shape of the lattice contribution should be but a fair estimate of the magnitude of that contribution.

For both types of structures investigated here more information would

be helpful if detailed calculations of the various contributions to the heat capacity of the other lanthanide-lead compounds are to be made. Specifically data from YPb_3 , in the normal state, would help establish what the effect of changing the mass of the lanthanide element has on the lattice contribution as would the data for Y_5Pb_3 and Lu_5Pb_3 . These data would also provide more information about the usefulness of Bijl's and other reduced representations.

CONCLUSIONS

This investigation has provided the electronic and lattice contributions to the heat capacity for the 1:3 and 5:3 lanthanide-lead compounds. Work on other compounds in these series would produce more accurate estimates of these contributions for the trivalent lanthanide-lead compounds with magnetic moments. The methods used to compare the results for YPb_3 and LaPb_3 show that the results for YPb_3 are reasonable but any doubt could be dispelled by measuring the heat capacity of YPb_3 in the normal state. Fitting the heat capacities with various models proposed by other investigators did not provide any explanations as to how or why the actual distribution of lattice vibrations, $g(\nu)$, varies with the frequency, (ν) . Bijl's reduced representation provides information on the extent of the deviation from Debye's model of the lattice contribution to the heat capacity of alloys but some of the observations of the influence of mass and anisotropy on the lattice contribution of elements do hold for alloys while others do not. Although more investigation is needed his reduced representation apparently shows that isostructural compounds should have reduced lattice heat capacities that are very similar.

BIBLIOGRAPHY

1. O. D. McMasters and K. A. Gschneidner, Jr., *Trans. Met. Soc. AIME* 239, 781 (1967).
2. O. N. Carlson, F. A. Schmidt and D. E. Diesburg, *Trans. Quart. ASM* 60, 119 (1967).
3. O. D. McMasters and K. A. Gschneidner, Jr., *J. Less-Common Metals* 13, 193 (1967).
4. O. D. McMasters, T. J. O'Keefe and K. A. Gschneidner, Jr., *Trans. Met. Soc. AIME* 242, 936 (1968).
5. O. D. McMasters, S. D. Soderquist and K. A. Gschneidner, *Trans. Quart. ASM* 61, 435 (1968).
6. J. T. Demel and K. A. Gschneidner, Jr., *J. Nucl. Materials* 29, 111 (1969).
7. O. D. McMasters and K. A. Gschneidner, Jr., *J. Less-Common Metals* 19, 337 (1969).
8. R. B. Griffin and K. A. Gschneidner, Jr., *Met. Trans.* 2, 2517 (1971).
9. O. D. McMasters and K. A. Gschneidner, Jr., to be published.
10. W. Jeitschko and E. Parthé, *Acta Cryst.* 19, 275 (1965).
11. W. Jeitschko, H. Nowotny and F. Benesovsky, *Monatsh. Chem.* 95, 1040 (1964).
12. A. Palenzona and M. L. Fornasini, *Atti accad. nazl. Lincei Rend.* 40, 1040 (1966).
13. W. Jeitschko and E. Parthé, *Acta Cryst.* 22, 551 (1967).
14. E. Franceschi, *J. Less-Common Metals* 22, 249 (1970).
15. F. Merlo and M. L. Fornasini, *Atti accad. nazl. Lincei Rend.* 46, 265 (1969).
16. A. Rossi, *Atti accad. nazl. Lincei Rend.* 17, 839 (1933).
17. R. J. Gambino, N. R. Stemple and A. M. Toxen, *J. Phys. Chem. Solids* 29, 295 (1968).
18. E. Zintl and S. Neumayr, *Z. Electrochem.* 39, 86 (1933).

19. F. Ruggiero and G. L. Olcese, *Atti accad. nazl. Lincei Rend.* 37, 169 (1964).
20. A. Rossi, *Gazz. chim. Ital.* 64, 832 (1934).
21. A. Iandelli, Paper No. 3F in "The Physical Chemistry of Metallic Solutions and Intermetallic Compounds," Her Majesty's Stationery Office, London (1959).
22. Yu. B. Kuzma, R. V. Skolozdra and V. Ya. Markiv, *Dopovidi Akad. Nauk Ukr. RSR* 1964, 1070.
23. A. Palenzona, *J. Less-Common Metals* 10, 290 (1966).
24. A. Iandelli, *Atti accad. nazl. Lincei Rend.* 29, 62 (1960).
25. G. Bruzzone and A. F. Ruggiero, *Atti accad. nazl. Lincei Rend.* 33, 465 (1962).
26. K. A. Gschneidner, Jr. and O. D. McMasters, *Monatsh. Chem.* 102, 1499 (1971).
27. E. Bucher, K. Andres, J. P. Maita and G. W. Hull, Jr., *Helv. Chim. Acta* 41, 723 (1968).
28. E. E. Havinga, *Phys. Rev. Letters* 28A, 350 (1968).
29. E. E. Havinga, H. Damsma and M. H. Van Maaren, *J. Phys. Chem. Solids*, 31, 2653 (1970).
30. E. S. R. Gopal, Specific Heats at Low Temperatures (Plenum, New York, 1966).
31. D. Hohnke and E. Parthé, *J. Less-Common Metals* 17, 296 (1969).
32. W. Rieger, H. Nowotny and F. Benesovsky, *Monatsch. Chem.* 96, 98 (1965).
33. H. Nowotny and F. Benesovsky, in Phase Stability in Metals and Alloys, edited by P. S. Rudman, J. Stringer, and R. I. Jaffee (McGraw-Hill Book Co., New York, 1967), Part 3, Chap. 6, p. 322.
34. N. T. Panousis, Ph.D. thesis (Iowa State University, 1970) (unpublished); also available as U.S. Atomic Energy Commission Report No. IS-T-398, 1970 (unpublished).
35. R. R. Joseph, Ph.D. thesis (Iowa State University, 1968) (unpublished); also available as U.S. Atomic Energy Commission Report No. IS-T-228, 1968 (unpublished).

36. J. S. Rogers, R. J. Tainsh, M. S. Anderson and C. A. Swenson, *Metrologia*, 4, 47 (1968).
37. D. W. Osborne, H. E. Flotow, and F. Schreiner, *Rev. Sci. Instr.* 38, 159 (1967).
38. N. T. Panousis and R. E. Hungsberg, Private Communication.
39. R. R. Joseph, K. A. Gschneidner, Jr. and D. C. Koskimski, *Phys. Rev. B* 6, 3286 (1972).
40. R. E. Hungsberg and K. A. Gschneidner, Jr., *J. Phys. Chem. Solids* 33, 401 (1972).
41. N. F. Mott and H. Jones, *The Theory of Metals and Alloys*, (Dover, New York, 1936).
42. W. deSorbo, *Acta Met.* 2, 274 (1954).
43. D. Bijl, in *Progress in Low Temperature Physics*, Vol. II, edited by C. J. Gorter (North-Holland Publ. Co., Amsterdam, 1957) Chap. 13, p. 395.
44. R. E. Hungsberg, M.S. Thesis (Iowa State University, 1969) (unpublished).

ACKNOWLEDGMENTS

No research can be done by one person and I would like to thank those that helped me or contributed in one way or another to this research project.

Dr. Gschneidner helped me define the problem and then had the patience to help me finish the work. Bob Joseph and Nick Panousis built the original calorimeter and modified it. Dave Koskimski, Jim Tonnie, Bill Taylor, Mike Hurley and Brent Haskell contributed help and/or discussions when needed. Paul Palmer and John Croat prepared the rare earth metals and Harlan Baker helped with the metallography. Jerry Ostenson provided the resistivity electronics and helped with the resistivity measurements. Dale McMasters helped with both information and programs for the X-ray work. Jack Moorman, Jim Holl and Howard Hensch all contributed both time and knowledge for a variety of small problems. My family was both encouraging and patient; without them this project could not have been started much less completed.

APPENDIX

Table A (1). Heat capacity of YPb_3

T (deg K)	C (mJ/g-at K)	T (deg K)	C (mJ/g-at K)
2.744	27.76	9.777	1082.72
3.045	42.83	9.959	1141.66
3.505	62.34	10.081	1183.49
3.886	88.58	10.365	1280.34
4.212	104.06	10.478	1243.41
4.429	123.45	10.848	1425.11
4.562	136.70	10.968	1487.69
4.746	126.51	11.277	1625.08
4.800	129.93	11.459	1666.33
5.022	148.61	11.664	1765.27
5.034	154.01	11.858	1808.40
5.365	180.47	12.192	1919.90
5.386	181.72	12.298	2001.50
5.640	208.66	12.813	2211.32
5.827	231.23	12.814	2232.95
5.958	240.77	13.237	2423.48
6.209	275.36	13.275	2453.55
6.211	278.52	13.638	2662.81
6.464	316.44	13.802	2669.64
6.499	320.18	14.224	2964.18
6.723	359.16	14.303	2971.46
6.789	366.10	14.817	3249.97
7.045	411.07	14.854	3283.64
7.112	422.62	15.314	3503.35
7.353	468.01	15.456	3599.18
7.420	483.19	15.906	3793.37
7.658	530.37	16.086	3998.76
7.771	547.08	16.500	4186.54
7.987	604.22	16.711	4316.57
8.135	632.08	17.120	4499.56
8.332	679.35	17.449	4699.25
8.504	722.44	17.837	4871.70
8.708	776.00	18.142	5148.89
8.915	840.03	18.537	5395.73
9.074	866.25	18.834	5611.25
9.437	980.81	19.325	5896.81
9.446	975.66		

Table A (2).. Heat capacity of LaPb_3

T (deg K)	C (mJ/g-at K)	T (deg K)	C (mJ/g-at K)	T (deg K)	C (mJ/g-at K)
2.619	22.02	5.422	139.54	10.621	1260.17
2.642	25.51	5.576	152.13	10.929	1351.88
2.653	23.15	5.681	161.45	11.092	1431.45
2.866	29.14	5.781	169.72	11.392	1542.02
2.977	27.78	5.968	189.78	11.513	1584.63
2.999	35.04	6.002	193.65	11.889	1731.47
3.183	39.90	6.166	212.65	11.990	1791.14
3.275	43.91	6.245	220.17	12.320	1908.43
3.328	49.80	6.255	222.13	12.462	1977.14
3.483	50.78	6.475	248.69	12.789	2123.61
3.541	60.50	6.490	252.61	12.878	2160.95
3.625	55.66	6.514	255.03	13.371	2331.97
3.738	61.23	6.752	288.69	13.404	2418.50
3.823	63.39	6.793	289.67	13.949	2664.72
3.945	72.31	7.039	330.63	13.997	2679.09
3.995	76.26	7.069	336.06	14.509	2926.36
4.017	76.26	7.366	385.74	14.562	2999.24
4.124	93.90	7.419	395.43	15.110	3334.20
4.188	60.22	7.731	453.09	15.116	3271.22
4.361	74.58	7.802	465.17	15.774	3609.69
4.378	76.31	8.122	531.59	15.788	3659.99
4.549	78.37	8.152	540.84	16.455	3952.62
4.659	84.08	8.533	628.57	16.540	4066.98
4.757	90.07	8.533	624.93	17.187	4384.00
4.826	87.54	8.907	723.81	17.199	4347.69
4.854	102.59	8.948	738.64	17.868	4826.02
4.914	102.48	9.286	832.75	17.908	4681.90
5.038	109.46	9.407	860.29	18.584	5245.47
5.104	114.45	9.741	957.73	18.623	5191.25
5.247	124.28	9.960	1030.25	19.326	5623.10
5.248	125.50	10.196	1122.89	19.365	5602.11
5.418	138.32	10.478	1191.58		

Table A (3). Heat capacity of La_5Pb_3 I

T (deg K)	C (mJ/g-at K)	T (deg K)	C (mJ/g-at K)	T (deg K)	C (mJ/g-at K)
2.675	11.36	6.613	226.16	11.906	1221.23
2.713	13.43	6.851	251.20	12.296	1372.21
3.127	18.86	6.956	261.05	12.458	1396.79
3.131	18.69	7.142	279.84	12.844	1510.05
3.508	27.65	7.262	298.21	12.844	1476.03
3.517	22.98	7.440	317.75	13.234	1682.02
3.797	34.42	7.598	348.81	13.253	1670.25
3.873	31.52	7.751	367.73	13.654	1765.69
4.159	47.10	7.971	403.44	13.734	1736.15
4.188	45.89	8.098	415.85	14.211	1986.10
4.482	63.58	8.391	470.64	14.359	2077.26
4.552	66.80	8.507	477.00	14.668	2123.23
4.728	70.22	8.872	554.53	14.868	2296.86
4.854	83.04	8.995	561.78	15.204	2316.53
5.003	90.80	9.281	626.78	15.453	2460.26
5.194	105.40	9.486	683.99	16.005	2642.64
5.221	105.38	9.619	692.78	16.176	2746.47
5.453	124.95	9.922	737.91	16.908	2986.11
5.461	124.44	9.967	774.53	16.948	3033.33
5.759	151.06	10.333	845.04	17.773	3334.06
5.764	147.79	10.348	832.07	17.811	3407.37
6.013	166.57	10.746	961.31	18.609	3723.14
6.042	168.48	10.835	961.69	18.762	3744.73
6.291	188.42	11.186	1061.41	19.419	4090.47
6.293	198.40	11.355	1071.69	19.629	4161.10
6.544	216.95	11.717	1210.82		

Table A (4). Heat capacity of La_5Pb_3 II

T (deg K)	C (mJ/g-at K)	T (deg K)	C (mJ/g-at K)
2.575	12.05	5.096	98.35
2.597	12.81	5.155	104.84
2.606	12.31	5.177	109.99
2.682	14.44	5.226	110.06
3.188	20.01	5.332	118.28
3.217	24.80	5.363	118.98
3.243	20.37	5.383	121.75
3.289	27.16	5.419	122.33
3.626	32.52	5.557	136.69
3.670	32.16	5.574	136.57
3.727	34.76	5.610	140.69
3.780	37.65	5.680	142.42
3.922	37.91	5.777	155.18
3.990	46.37	5.808	155.07
4.057	49.12	5.833	160.64
4.071	46.45	5.961	167.07
4.171	46.90	6.009	174.80
4.265	58.28	6.040	177.19
4.292	58.31	6.063	179.45
4.383	54.48	6.194	189.30
4.403	56.58	6.254	197.48
4.485	68.29	6.274	198.09
4.512	70.59	6.316	206.46
4.608	66.79	6.408	211.86
4.662	72.80	6.525	224.99
4.679	78.66	6.655	237.78
4.766	84.78	6.782	250.73
4.826	82.80	6.916	268.61
4.878	92.93	7.057	288.32
4.920	85.05	7.197	302.70
4.964	96.28	7.331	317.11
5.047	99.04		

Table A(5). Heat capacity of $\text{La}_5\text{Pb}_3\text{C}$

T (deg K)	C (mJ/g-at K)	T (deg K)	C (mJ/g-at K)	T (deg K)	C (mJ/g-at K)
2.588	10.39	6.162	113.02	10.942	822.50
2.634	9.33	6.192	118.28	11.251	909.49
2.797	11.85	6.344	129.63	11.435	939.58
3.089	13.76	6.487	138.61	11.538	982.78
3.136	15.18	6.513	145.06	11.881	1054.43
3.204	14.53	6.733	168.29	11.911	1087.45
3.289	15.99	6.828	173.52	12.338	1148.55
3.496	20.82	6.919	190.96	12.361	1157.27
3.607	20.54	7.125	208.13	12.786	1306.61
3.620	21.64	7.187	208.88	12.882	1320.33
3.831	23.61	7.363	235.85	13.221	1446.80
3.903	26.16	7.505	242.91	13.465	1516.35
3.948	26.70	7.627	261.86	13.756	1602.67
4.017	28.02	7.829	282.88	14.045	1719.91
4.136	32.62	7.891	296.26	14.393	1799.15
4.316	29.43	8.173	333.75	14.628	1905.02
4.353	32.50	8.214	330.05	15.058	2078.92
4.399	35.41	8.451	375.44	15.182	2093.30
4.414	38.02	8.617	390.94	15.679	2287.26
4.566	41.64	8.765	420.11	15.773	2314.91
4.635	45.59	9.013	457.65	16.379	2601.56
4.832	50.97	9.041	451.63	16.387	2579.44
4.885	51.63	9.305	512.72	17.045	2842.76
5.093	61.00	9.462	527.77	17.151	2933.75
5.236	63.56	9.646	560.04	17.746	3130.57
5.303	78.91	9.945	620.70	18.055	3269.21
5.507	80.92	9.977	634.67	18.401	3481.73
5.552	84.57	10.268	683.11	19.058	3816.79
5.686	86.90	10.430	711.01	19.087	3851.62
5.859	99.32	10.570	751.93	19.732	4208.15
5.886	100.73	10.927	837.05	20.025	4378.06
6.005	104.26				